

A Compact Planar Low-Pass Filter Based on SRR-Metamaterial

Badr Nasiri¹, Ahmed Errkik², Jamal Zbitou³, Abdelali Tajmouati⁴, Larbi El Abdellaoui⁵,
Mohamed Latrach⁶

^{1, 2, 3, 4, 5}LMEET FST of Settat, Hassan 1st University, Morocco

⁶Microwave Group (ESEO), France

Article Info

Article history:

Received Jan 23, 2018

Revised Jul 24, 2018

Accepted Aug 6, 2018

Keyword:

Low-pass filter

Metamaterial

Microstrip

SRR

ABSTRACT

In this work, a novel design of a Microstrip Low-pass filter based on metamaterial square split ring resonators (SRRs) is proposed. The SRRs has been added to obtain a reduced size and high performances. The filter is designed on an FR-4 substrate having a thickness of 1.6mm , a dielectric constant of 4.4 and loss tangent of 0.025 . The proposed low-pass filter is characterized by a cutoff frequency of 2.4 GHz and an attenuation level below than -20dB in the stopband. The LPF is designed, simulated and optimized by using two electromagnetic solvers CST microwave studio and ADS. The computed results obtained by both solvers are in good agreement. The total surface area of the proposed circuit is $18\times 18\text{mm}^2$ excluding the feed line, its size is miniaturized by 40% compared to the conventional filter. The experimental results illustrate that the filter achieves very good electrical performances in the passband with a low insertion loss of 0.2 dB . Moreover, a suppression level can reach more than 35 dB in the rejected band.

Copyright © 2018 Institute of Advanced Engineering and Science.
All rights reserved.

Corresponding Author:

Badr Nasiri,

LMEET FST of Settat,

Hassan 1st University, Settat, Morocco,

BP : 577, Route de Casablanca, Settat, Morocco.

Email : b.nasiri@uhp.ac.ma

1. INTRODUCTION

Filters are one of the most important components in microwave systems. These are used to control the frequency response at a certain point by allowing a particular range of frequencies or blocking undesired signals [1]. On the basis of its frequency response, the filter can be classified as high pass, low-pass, band-reject and a band-pass filter. The low pass filter only allows passing the low-frequency signals from 0Hz to its cut-off frequency, while attenuating high-frequency signals [1]-[4].

Recently, the demand for the microstrip low pass filters in wireless and mobile communication systems has rapidly increased due to its low cost, low insertion loss, ease of integration and compatibility with planar fabrication processes. Conventional microwave low-pass filter with open stub and stepped impedance are used for their excellent characteristics. However, filters with small size and high performance are widely desired and difficult to achieve. Therefore, several techniques have been used by many researchers such as defected ground structures (DGSs) method, fractal geometry, and metamaterials in order to reduce the microstrip filter dimensions [2]-[13].

In the late 1960s, metamaterials were firstly introduced by the Russian physicist Victor Veselago. They are artificial electromagnetic materials that do not exist in nature and have a negative permittivity, negative permeability or simultaneously negative permittivity and negative permeability. These materials take their unusual characteristics from their structures rather than their compositions. In applied microwave field, there are numbers of metamaterial types that can be useful in microstrip low-pass filters such as split

ring resonators (SRRs) were proposed by Pendry in 1999, Complementary split ring resonators (CSRRs) were proposed by Falcone in 2004 and Complementary hexagonal-omega structures [6], [8]-[16].

In this paper, we present a microstrip low-pass filter based on SRRs metamaterial, this filter is designed to have a desired cut-off frequency of 2.4 GHz and a reflection coefficient under -22dB in the bandwidth in order to achieve an excellent transmission in this range of frequencies.

2. THEORY AND DESIGN PROCEDURE

2.1. Conventional Open Stubs Low-pass Filter

For comparison purposes, the conventional low-pass filter using open stubs was designed on FR-4 substrate and its performance was carried out using ADS Agilent. Firstly, the 3rd order Butterworth low-pass filter has been chosen in order to achieve a maximally flat response, desired bandwidth and a cutoff frequency of 2.4 GHz that shown in Figure 1..

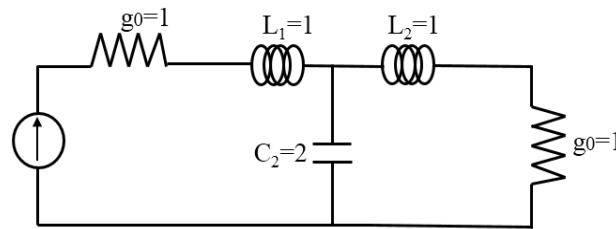


Figure 1. Lumped-element of 3rd order butterworth low-pass filter prototype

Secondly, Richard's transformation was used to convert lumped inductors into short circuit stubs and shunt capacitors to open circuit stubs can see in Figure 2. For the line length $l = \lambda_0/8$ at a particular reference frequency $f_0 = V_p / \lambda_0$, we have:

$$j\omega L = jZ_0 \tan\left(\left(\frac{\pi}{4}\right)\Omega\right) = SZ_0 \tag{1}$$

$$j\omega L = jZ_0 \tan\left(\left(\frac{\pi}{4}\right)\Omega\right) = SZ_0 \tag{2}$$

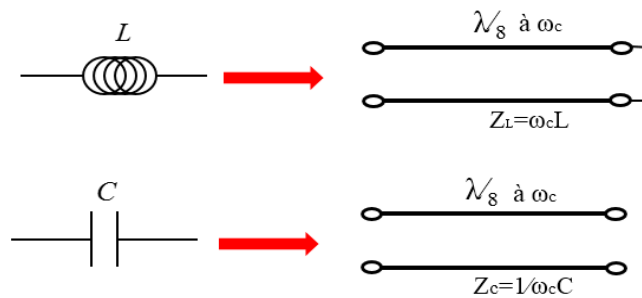


Figure 2. Richards' transformation for an inductor to a short-circuit stub and for capacitor to an open stub

By employing the Kuroda identities, we can also convert short-circuit stubs into open-circuit stubs. The calculated impedances of transmission line segment and open stubs are shown in Figure 3 (a). Figure 3 (b) illustrates the obtained conventional microstrip low-pass filter layout using open stubs.

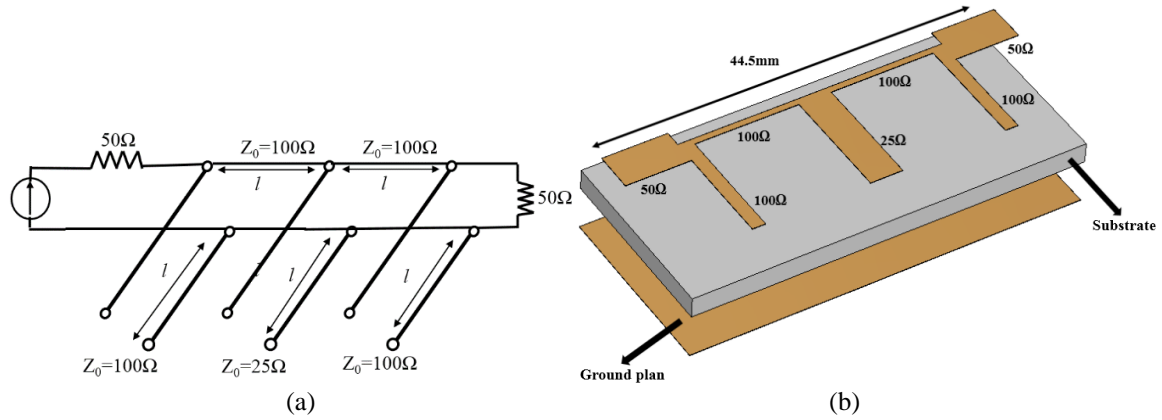


Figure 3. (a) The conventional LPF after impedance and frequency scaling, (b) layout of the conventional LPF

The physical width and length of the microstrip lines have been calculated to obtain a desired cut-off frequency of 2.4 GHz, the overall results are listed in Table 1.

Table 1. Width and Length Dimensions of LPF

Z(Ω)	W (mm)	L (mm)
100	0.67	9.08
50	3.05	8.57
25	8.42	8.14

Figure 4 demonstrates the frequency response of the conventional low pass filter, the simulated transmission and reflection parameters are obtained by using ADS Agilent.

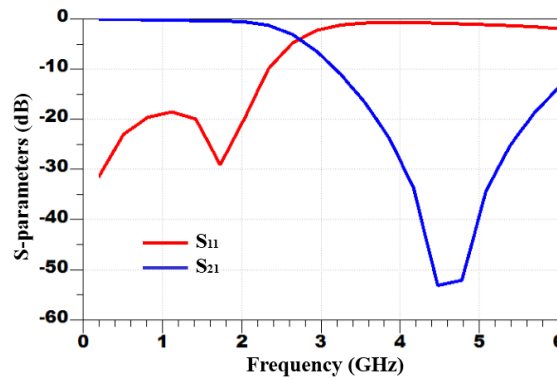


Figure 4. Frequency response of the conventional LPF

2.2. The Proposed Low-pass Filter Based on Metamaterials.

The proposed low-pass filter design approach begins with a simple small microstrip structure compounded of two stubs and a transmission section line connected to 50Ω in/out port. In the second part, the square split ring resonators (SRRs) are added to achieve the desired cut-off frequency and LPF compact size.

To obtain good electrical performances from the proposed LPF, various SRR-parameters were tuned and optimized using CST Microwave based on finite element method. The layout of the proposed low pass filter without SRRs is shown in Figure 5, it has an overall size of 18x18mm² without 50 Ω conductor line.

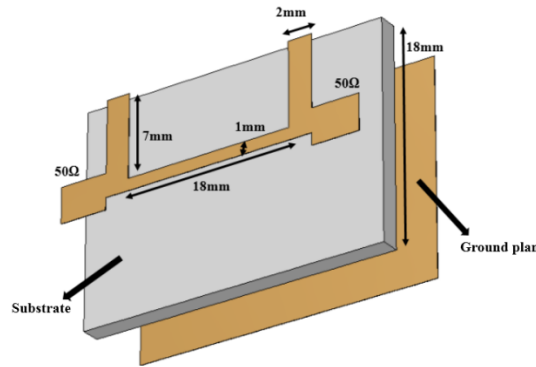


Figure 5. Layout of the proposed filter without SRRs

The equivalent circuit of the LPF without SRRs is shown in Figure 6 (a) and the simulated results are performed by using ADS Agilent. The simulated S-parameter of the LC equivalent circuit and layout of the proposed LPF without SRRs are presented in Figure 6 (b). According to the simulated results, we can observe that the attenuation is weak in the stopband.

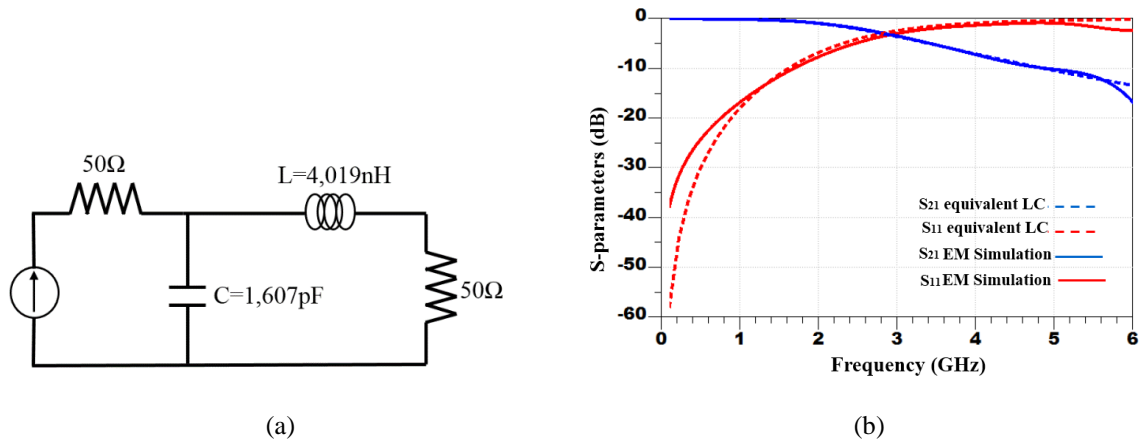


Figure 6. (a) Equivalent circuit of proposed filter without SRRs, (b) frequency response of the LC equivalent circuit and layout

To increase the attenuation level (S_{21}) in the stopband and to obtain the desired cut-off frequency of 2.4 GHz, the square split ring resonators (SRRs) are loaded into the structure. The square split ring resonator unit cell is compounded by two concentric square metallic rings on opposing sides. It can be represented by an electrical circuit model [17]. The SRR behaves as LC circuit and approximated by using four distributed inductors L_1, L_2, L_3 and L_4 where $L_2=L_4$ that is produced by one side integrated outer and inner current sheet. L_1 and L_3 represent the self-inductors produced by an integrated sheet and a sheet with the opening, as well as four distributed capacitances that are divided into two parts, the first one is the coupling capacitance between both rings and the second part is produced by the electric charges accumulated at the opening of the two rings. Figure 7 shows respectively the SRR and its equivalent LC circuit [17].

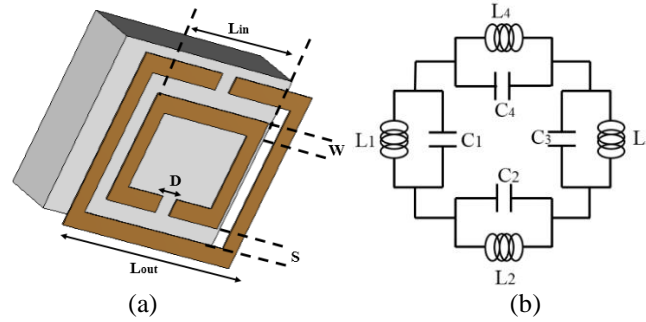


Figure 7. (a) The SRR unit cell, (b) SRR Equivalent LC circuit

where.

$$L_2 = L_4 = \frac{\mu_0 n^2 L_{out}}{2\pi} \left[\ln\left(\frac{2}{\rho}\right) + 0.5 + 0.178\rho + 0.0146\rho^2 + \frac{0.5(n-1)S^2}{(\rho n)^2} + 0.178 \frac{(n-1)S}{n} - \frac{1}{n} \ln\left(\frac{W+t}{W}\right) \right] \quad (3)$$

$$\rho = \frac{nW + (n-1)S}{L_{out}} \quad (4)$$

L_{out} : The length of out ring sides.

W : The metal width.

S : The space between inner and outer rings.

n : The number of turns.

t : the vertical parameter of SRR.

$$L_1 = L_3 = K \frac{\mu_0 n^2 L_{out}}{2\pi} \left[\ln\left(\frac{2}{\rho}\right) + 0.5 + 0.178\rho + 0.0146\rho^2 + \frac{0.5(n-1)S^2}{(\rho n)^2} + 0.178 \frac{(n-1)S}{n} - \frac{1}{n} \ln\left(\frac{W+t}{W}\right) \right] \quad (5)$$

$$K = \frac{(2L - 2S) - D}{(2L - 2S)} \quad (6)$$

$$C_2 = C_4 = \frac{1}{4} \left[0.06 + 3.5 \times 10^5 (r_{out} + r_{in}) \right] \quad (7)$$

$$C_3 = \frac{1}{4} \left[0.06 + 3.5 \times 10^5 (r_{out} + r_{in}) \right] + \frac{3\epsilon_0 S}{D} \quad (8)$$

$$C_1 = \frac{1}{4} \left[0.06 + 3.5 \times 10^5 (r_{out} + r_{in}) \right] + \frac{25\epsilon_0 S}{D} \quad (9)$$

r_{out} : the radius of the outer circumcircle

r_{in} : the radius of the inner circumcircle

$L_{out} = 6mm, L_{in} = 4mm$ and $D = S = W = 0.5mm$.

The chosen square split ring resonator is simulated and the existence of the negative permeability was carried out by using The S-parameter Retrieval. This technic is extensively used to extract effective medium parameters from the simulated scattering responses. Contrariwise, the analytical techniques are difficult to apply in order to calculate the medium parameters. The effective permittivity and permeability are related to the simulated transmission S_{21} and reflection S_{11} by following equations

$$n = \frac{1}{k_0 d} \cos^{-1} \left[\frac{1}{2S_{21}} (1 - S_{11}^2 + S_{21}^2) \right] \tag{10}$$

$$z = \pm \sqrt{\frac{(1 + S_{11})^2 + S_{21}^2}{(1 - S_{11})^2 + S_{21}^2}} \tag{11}$$

$$\epsilon_{eff} = \frac{n}{z} \tag{12}$$

$$\mu_{eff} = nz \tag{13}$$

Figure 8 (a) and Figure 8 (b) present respectively the simulated S-parameters of the chosen SRR unit cell and, calculated real and imaginary effective permeability against frequency. As might be seen in figure below, metamaterial unit cell has a negative value of the permeability around of its resonant frequency.

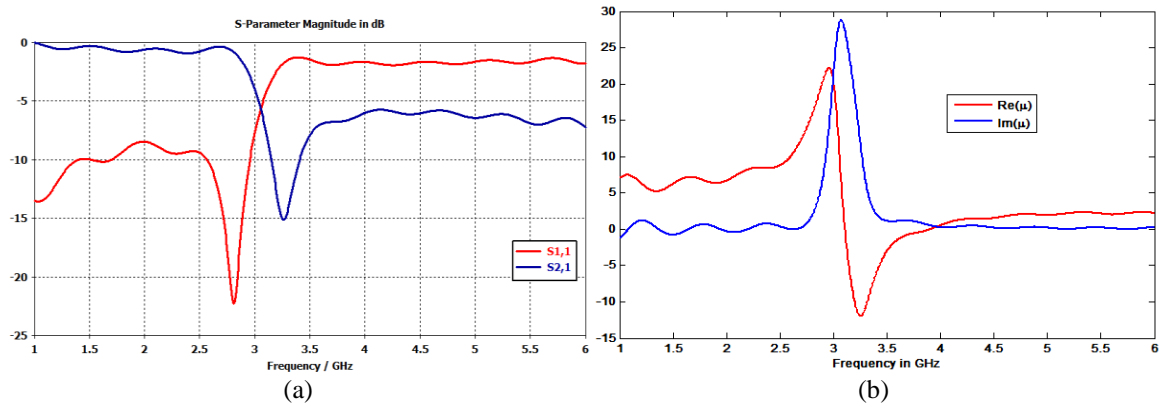


Figure 8. (a) simulated S-parameters of the SRR unit cell, (b) Effective permeability of SRR unit cell

To improve the out-band suppression and to achieve a good insertion and return loss in the bandwidth, the SRRs have been added close to the microstrip line structure, where the distance between the resonator and the microstrip line is 0.5 mm. The final proposed LPF is illustrated in Figure 9.

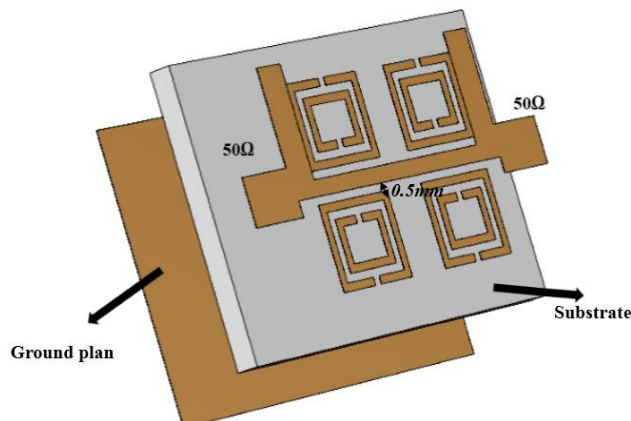


Figure 9. Layout of the final proposed microstrip low pass filter

The simulated S-parameters of the proposed low-pass filter are illustrated in Figure 10. According to this figure, the cut-off frequency of the LPF is found to be 2.4 GHz. In comparison with the initial structure, the final LPF has a higher attenuation level in the stopband below than -20dB, a good performance in the passband compared to the proposed filter without SRRs and more than 40% miniaturization compared to the conventional microstrip low-pass filter. To validate the simulated results achieved by CST Microwave Studio and before the manufacturing processes, another simulation has been carried out by using ADS Agilent. Figure 10 shows the computed obtained results by CST Microwave Studio and ADS Agilent. As can be seen, good agreement between the both simulations results obtained by two electromagnetic solvers.

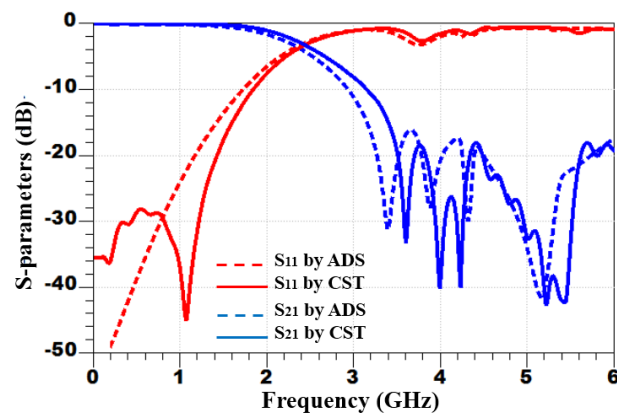


Figure 10. Frequency response of the proposed LPF by using CST Microwave studio and ADS Agilent

Figure 11 describes the surface current results of the designed LPF in the pass band at 1.5GHz and in the stop-band at 4.5GHz. As noted in the figure, a maximum current is shown around the metamaterial resonators in the stopband and no current close to the output port which proves that there is no transmission of the RF power between the input port and output port. At 1.5 GHz the maximum current is located on the microstrip transmission line which implies that there is a propagation of radio frequency power on the proposed circuit.

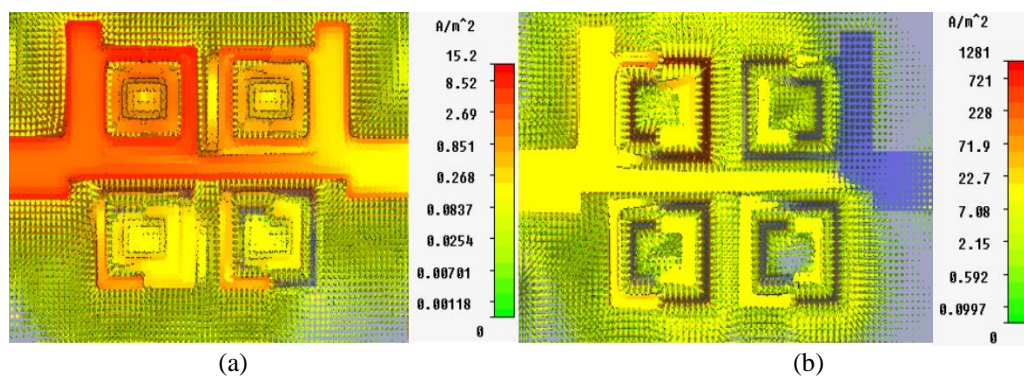


Figure 11. (a) Surface current at 1.5GHz, (b) Surface current at 4.5GHz

3. ACHIEVEMENT AND MEASUREMENT

After the validation of simulation, the proposed filter was fabricated on a 1.6 mm thick FR4 substrate described in design phase and the measurements were achieved by an R&S Vector Network Analyzer. The filter dimensions remain the same as those presented in Figure 5 and 9. The fabricated LPF prototype photograph is illustrated in Figure 12 (a).

Figure 12 (b) shows the simulated and measured S-parameters results of the proposed LPF based on SRRs, which are in excellent agreement. It can be distinctly seen that this proposed filter with -3dB cut-off of 2.4 GHz has a low insertion loss of 0.2 dB from DC to 1.8 GHz and the value of return loss in this range is

higher than 20 dB, which implies good electrical performances in the passband. The stopband insertion loss shows a power rejection that can reach more than 35 dB. The slight change in the value of rejected-band return loss is mainly due to the dielectric losses and fabrication errors.

This filter offers high performances in terms of size, passband insertion loss plus return loss, and stopband rejection level. The filter with these features is a suitable for many applications in modern communication systems.

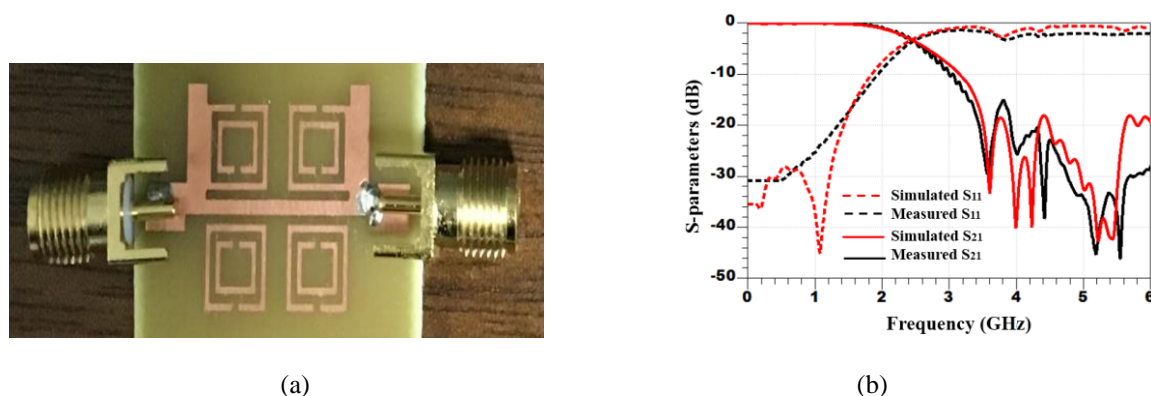


Figure 12. (a) Fabricated LPF, (b) Simulated and measured S-parameters of the proposed LPF

4. CONCLUSION

A novel microstrip low-pass filter based on square split ring resonator was designed and optimized by using CST Microwave studio. This proposed LPF characterized by a cutoff frequency of 2.4 GHz has good characteristics such as higher attenuation level in the stopband and good return loss in the passband. The size of LPF is miniaturized by 40% compared to the conventional filter. It is an adequate solution for communication systems in GSM, DCS and UMTS bands.

ACKNOWLEDGEMENTS

We would like to thank Mr. Mohamed LATRACH Professor in ESEO, Engineering Institute in Angers, France, for allowing us to use all the equipments and solvers available in his laboratory.

REFERENCES

- [1] D. M. Pozar, "Microwave Engineering," 3rd ed., Wiley, Inc., 2005.
- [2] S. H. Fu, *et al.*, "Compact Miniaturized Stepped Impedance Lowpass Filter with Sharp Cutoff Characteristic," *Microwave and Optical Technology Lett.*, vol/issue: 51(10), pp. 2257-2258, 2009.
- [3] M. Hayati, *et al.*, "Microstrip Lowpass Filter with High and Wide Rejection Band," *IEE Electron. Lett.*, vol/issue: 48(19), pp. 1217-1219, 2012.
- [4] A. Rahman, *et al.*, "Control of Bandstop Response of Hi-Lo Microstrip Low Pass Filter Using Slot in Ground Plane," *IEEE Trans. Micro. Theory and Techniques*, vol/issue: 52(3), pp. 2539-2545, 2004.
- [5] A. F. Morabito, *et al.*, "Isophoric Array Antennas with a Low Number of Control Points: A 'Size Tapered' Solution," *Progress in Electromagnetics Research Letters*, vol. 36, pp. 121-131, 2013.
- [6] A. Ennajih, *et al.*, "A New Dual Band Printed Metamaterial Antenna for RFID Reader Applications," *International Journal of Electrical and Computer Engineering*, vol/issue: 7(6), pp. 3507-3514, 2017.
- [7] A. F. Morabito, "Power synthesis of mask-constrained shaped beams through maximally-sparse planar arrays Telkommnika," *TELKOMNIKA (Telecommunication Computing Electronics and Control)*, vol/issue: 14(4), pp. 1217-1219, 2016.
- [8] Y. Gaurav and R. K. Chauhan, "A Compact UWB BPF with a Notch Band using Rectangular Resonator Sandwiched between Interdigital Structure," *International Journal of Electrical and Computer Engineering IJECE*, vol/issue: 7(5), pp. 2420-2425, 2017.
- [9] B. Nasiri, *et al.*, "A Novel Design of a Compact Miniature Microstrip Low Pass Filter Based on SRR," *Proc. IEEE International Conference on Wireless Technologies, Embedded and Intelligent Systems (WITS)*, pp. 1-5, 2017.
- [10] F. Aznar, *et al.*, "Compact Lowpass Filters With Very Sharp Transition Bands Based on Open Complementary Split Ring Resonators," *Electron. Lett.*, vol/issue: 45(6), pp. 316-317, 2009.
- [11] Y. Yang, *et al.*, "Microstrip Lowpass Filter Based on Split Ring and Complementary Split Ring Resonators," *Microwave and Optical Technology Letters*, vol/issue: 54(7), pp. 1723-1726, 2012.

-
- [12] S. Sahu, *et al.*, “Compact Metamaterial Microstrip Low-Pass Filter,” *Journal of Electromagnetic Analysis and Applications*, vol/issue: 3(10), pp. 399-405, 2011.
- [13] B. Nasiri, *et al.*, “A New Compact and Wide-band Band-stop filter Using Rectangular SRR,” *TELEKOMNIKA (Telecommunication, Computing, Electronics and Control)*, vol/issue: 16(1), pp. 110–117, 2018.
- [14] B. Nasiri, *et al.*, “A New Compact Microstrip Band-stop Filter by Using Square Split Ring Resonator,” *International Journal of Microwave and Optical Technology*, vol/issue: 12(5), pp. 367-373, 2017.
- [15] J. B. Pendry, *et al.*, “Extremely Low Frequency Plasmons in Metallic Mesostructures,” *Phys. Rev. Lett.*, vol/issue: 76(25), pp. 4773-4776, 1996.
- [16] V. G. Veselago, “The Electrodynamics of Substances with Simultaneous Negative Values of ϵ and μ ,” *Soviet PhysicsUspekhi*, vol/issue: 10(4), pp. 509-514, 1968.
- [17] M. F. Wu, *et al.*, “A Compact Equivalent Circuit Model for The SRR Structure in Metamaterials,” *Microwave Conference Proceedings, 2005. Asia-Pacific Conference Proceedings APMC, 2005.*